



DOI: 10.58224/2618-7183-2026-9-2-3



## Polymeric composites and a study of the effect of ferrocene-based reinforcements on their mechanical properties

Puzin Y.I. \* <sup>1</sup> , Khabrat Gh.R. <sup>1</sup> 

<sup>1</sup> St. Petersburg Mining University of Empress Catherine II, Russia

**Abstract.** Polymer composites have become one of the most widely used and beneficial materials in modern industries due to their desirable structure, light weight, high strength, and flexibility. The positive role of these polymer composites is largely dependent on the size, structure, and dispersion phase of the reinforcing phase. In this article through a systematic review the influence of various parameters on the mechanical properties of polymer composites is analyzed, considering reinforcements based on ferrocene and ferrocene containing compounds. Different types of reinforcements, including fine particles (micro and nano), fibers (natural and synthetic), and two dimensional nanomaterials (such as graphene and inorganic compounds), have been investigated. The innovative role of reinforcements based on ferrocene and their derivatives is discussed in detail, highlighting their potential to simultaneously enhance mechanical, thermal and flame-retardant properties. The reinforcement mechanisms, including effective load transfer strong interfacial bonding, and crack bridging are described. Furthermore hybrid composites, which utilize a combination of multiple reinforcements to achieve superior properties, are reviewed. Analysis of recent studies indicates that ferrocene derivatives, with their unique sandwich structure, significantly improve interfacial adhesion through strong  $\pi$ - $\pi$  interactions and surface modification capabilities, often leading to a considerable increase in toughness and impact strength. Finally existing challenges and future perspectives including optimizing reinforcement dispersion and the development of smart ferrocene-based composites are discussed.

**Keywords:** polymer matrix composites, mechanical properties, ferrocene reinforcements, ferrocene compounds, hybrid composites, two-dimensional nanomaterials

**Please cite this article as:** Puzin Y.I., Khabrat Gh.R. Polymeric composites and a study of the effect of ferrocene-based reinforcements on their mechanical properties. Construction Materials and Products. 2026. 9 (2). 3. DOI: 10.58224/2618-7183-2026-9-2-3

\*Corresponding author E-mail: [ppuziny@mail.ru](mailto:ppuziny@mail.ru)

## 1. INTRODUCTION

Composite materials are formed by combining two or more dissimilar materials with different physical and chemical properties. The goal of this process is to obtain a material with new properties that are impossible to achieve from the individual components [1]. These materials consist of a continuous phase (matrix) and a discontinuous phase (reinforcement). Polymer matrix composites (PMCs) occupy a significant share of the composites market due to their low density high specific strength, corrosion resistance and ease of processing. The mechanical properties of (PMCs) depend significantly on the properties of each component and, in particular, on the quality of the interface between the matrix and the reinforcing element. The reinforcing elements bear the applied load while the matrix holds them in place and transfers the load between them. Therefore, the selection of the type, size, shape and amount of reinforcing elements is a critical design parameter.

In recent years advances in nanotechnology have revolutionized the field of composites, nanoreinforcements, owing to their very high surface to volume ratios, possess a unique ability to interact with the polymer matrix, resulting in significant improvements in mechanical, thermal, and even electrical properties at very low concentrations [2]. Among nanomaterials organometallic compounds have attracted considerable attention because they combine unique metallic and organic properties. Ferrocene (dicyclopentadienyl iron), one of the best known compounds in this family, exhibits exceptional thermal and chemical stability due to its unique sandwich structure. These properties make ferrocene and its derivatives ideal candidates for use as reinforcements in polymer composites. This article presents a systematic review of the effects of various types of reinforcements, with a particular emphasis on the less-studied potential of ferrocene-based reinforcements for the mechanical properties of polymer composites [3].

## 2. METHODS AND MATERIALS

The materials used in this study include various polymer matrices and ferrocene-based reinforcements. Table 1 summarizes the key materials, their specifications, and sources.

**Table 1.** List of materials used in the preparation and analysis of polymer/ferrocene composites.

| Material             | Chemical formula /specification      | Supplier/source  | Purity/properties               |
|----------------------|--------------------------------------|------------------|---------------------------------|
| Epoxy resin          | ED-20 (bisphenol a diglycidyl ether) | Khimprom, Russia | Epoxy equivalent: 20-22 g/eq    |
| Ferrocene            | $Fe(C_5H_5)_2$                       | Sigma-Aldrich    | $\geq 98\%$                     |
| Polyamide-6          | PA-6 (Granules)                      | BASF (Ultramid®) | Density: 1.13 g/cm <sup>3</sup> |
| Polypropylene        | PP (Homo-polymer)                    | Exxon Mobil      | MFI: 12 g/10 min                |
| Ferrocene derivative | Amino – ferrocene ( $Fe - NH_2$ )    | Synthesized      | $> 95\%$                        |
| Solvent              | Acetone ( $C_3H_6O$ )                | Vekton, Russia   | Analytical grade                |

### Preparation of Composites

The polymer composites were prepared by solution mixing method. The polymer matrix (epoxy resin or polyamide) was first dissolved in an appropriate solvent (acetone for epoxy, formic acid for polyamide) at  $50^\circ C$  under continuous stirring. Ferrocene or its derivatives were added to the solution at concentrations of 1, 3 and 5% wt. relative to the polymer mass. The mixture was stirred for 2 hours to ensure homogeneous dispersion, then cast into PTFE molds. For thermosetting matrices a hardener was added prior to casting, and the samples were cured at  $80^\circ C$  for 24 hours. For thermoplastic matrices, the solvent was evaporated at  $60^\circ C$  under vacuum for 48 hours [4].

### Characterization methods

*X-ray Diffraction (XRD)* – X-ray diffraction analysis was performed to investigate the crystalline structure of the composites and confirm the incorporation of ferrocene. An ARL PERFORM'X (thermo fisher scientific, USA) diffractometer was used with Cu-K $\alpha$  radiation ( $\lambda = 1.5406 \text{ \AA}$ ) at 40 kV

and 30 mA. Diffraction patterns were recorded in the  $2\theta$  range from  $5^\circ$  to  $70^\circ$  at a scanning rate of  $2^\circ/\text{min}$ . The interplanar spacing ( $d$ ) was calculated using Bragg's law:  $n\lambda = 2d \sin\theta$ .

*Scanning Electron Microscopy (SEM)* -The morphology of the composites and the dispersion state of ferrocene particles were examined by scanning electron microscopy using a JSM-7100F (JEOL, Japan) microscope. Samples were cryo-fractured in liquid nitrogen to obtain a fresh cross-sectional surface, then coated with a thin layer of gold ( $\approx 10$  nm) by sputtering to avoid charging effects. Images were taken at an accelerating voltage of 15 kV using secondary electron (SE) detectors.

*Mechanical testing* -Tensile properties were evaluated according to ASTM D638 standard using a Z020 universal testing machine (ZwickRoell, Germany). Dumbbell-shaped specimens (type V) were tested at a crosshead speed of 5 mm/min at room temperature ( $23 \pm 2^\circ\text{C}$ ). At least five specimens were tested for each composition, and the average values of tensile strength, elastic modulus, and elongation at break were reported.

Flexural strength was measured by three-point bending test following ASTM D790. Specimens with dimensions  $80 \times 10 \times 4$  mm were tested with a support span of 64 mm and a crosshead speed of 2 mm/min [5].

*Brunauer-Emmett-Teller (BET) Surface area analysis* – The specific surface area and pore characteristics of the composites were determined by nitrogen adsorption-desorption isotherms at  $-196^\circ\text{C}$  using an SSA-7000 analyzer. Samples were degassed at  $150^\circ\text{C}$  for 3 hours prior to measurement. The BET method was used to calculate surface area, while the Barrett-Joyner-Halenda (BJH) method was applied for pore size distribution.

Fig 1 presents a comprehensive set of characterization data for  $\alpha - \text{Fe}_2\text{O}_3$  catalysts with different iron isotopes, as reported in. These results are presented here for comparative purposes, as iron-based nanostructures share similar characteristics with ferrocene-based reinforcements. The figure includes:

a) XRD patterns - showing characteristic peaks at  $2\theta = 24.1^\circ, 33.2^\circ$ , and  $35.6^\circ$  corresponding to the (102), (104) and (110) planes of  $\alpha - \text{Fe}_2\text{O}_3$ . Understanding such crystalline features is essential for interpreting the structural behavior of iron-containing reinforcements in polymer composites.

b) SEM images – revealing irregular lump-shaped particles with rough surfaces containing pores and gullies. Such surface morphology is known to enhance mechanical interlocking with polymer matrices, leading to improved interfacial adhesion.

c) FTIR spectra – exhibiting characteristic **Fe – O** vibration peaks around  $560$  and  $430 \text{ cm}^{-1}$ . In ferrocene-based composites, similar metal-ligand vibrations can be observed, confirming the presence of organometallic structures.

d) UV-Vis diffuse reflectance spectra and corresponding tauc plots - demonstrating characteristic band gap values (1.73-1.97 eV) for iron-based materials which can serve as a reference for understanding the optical behavior of ferrocene-reinforced composites.

e) XPS spectra – showing Fe 2p peaks at approximately  $710.9 \text{ eV}$  ( $\text{Fe } 2p_{3/2}$ ) and  $724.4 \text{ eV}$  ( $\text{Fe } 2p_{1/2}$ ), characteristic of iron in oxide form. Similar binding energy values in ferrocene-based composites can indicate the presence of iron-centered structures.

f) Nitrogen adsorption-desorption isotherms and corresponding (BET) data – showing significantly higher surface areas (120-145  $\text{m}^2/\text{g}$ ) for iron oxide nanoparticles compared to typical polymer composites, highlighting their potential as high-surface-area reinforcements [6].

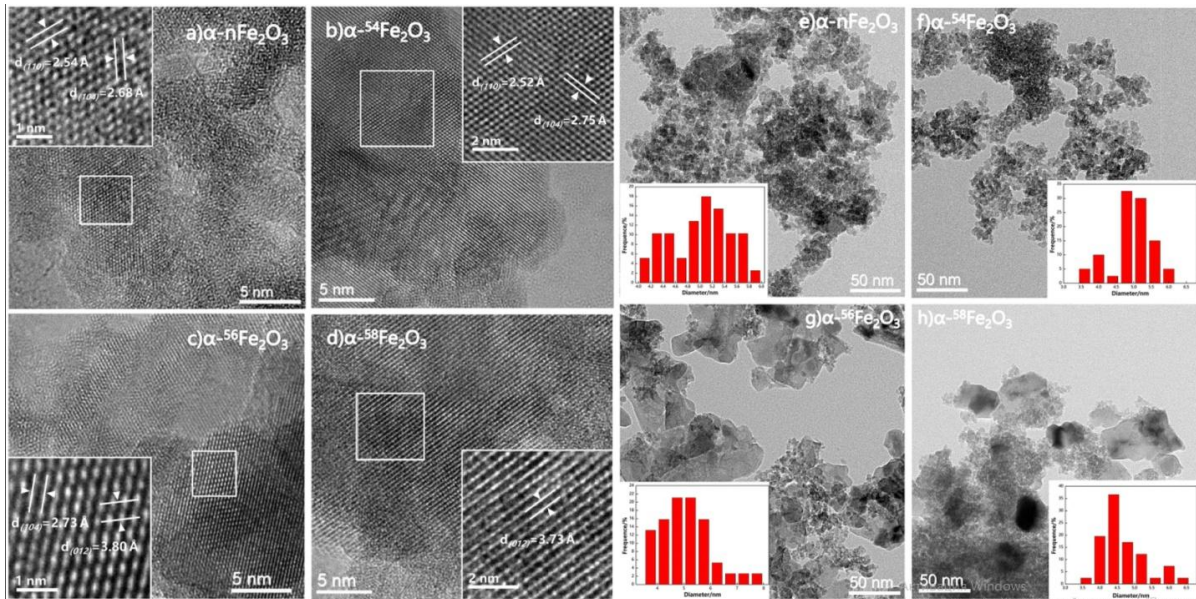


**Fig. 1.** Comprehensive characterization of  $\alpha - \text{Fe}_2\text{O}_3$  catalysts with different iron isotopes: (a) XRD patterns, (b) SEM images, (c) FTIR spectra, (d) UV-Vis DRS spectra and Tauc plots, (e) XPS spectra, and (f) nitrogen adsorption-desorption isotherms.

#### Fourier-Transform Infrared Spectroscopy (FTIR)

FTIR Spectra were recorded using a nicolet is10 spectrometer (Thermo Scientific, USA) in the range of  $4000 - 400 \text{ cm}^{-1}$  with a resolution of  $4 \text{ cm}^{-1}$ . Samples were prepared as KBr pellets. The spectra were used to identify chemical interactions between ferrocene and the polymer matrix [7].

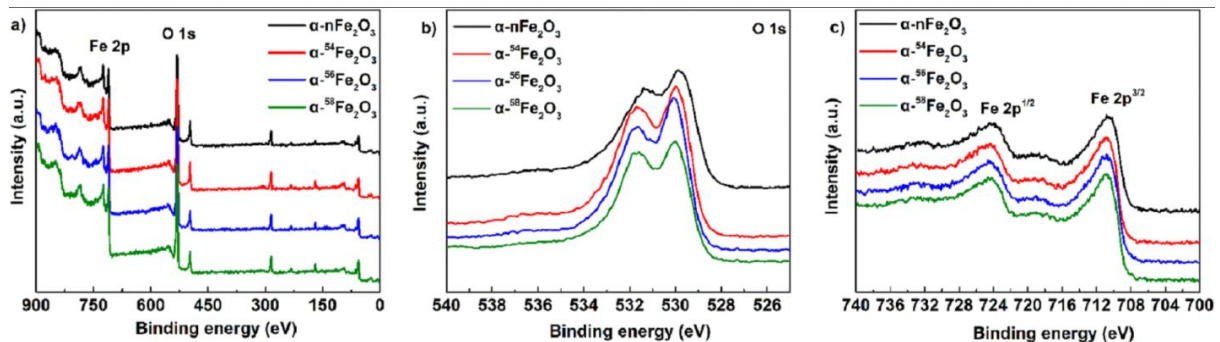


**Fig. 2.** FTIR spectra of  $\alpha - \text{Fe}_2\text{O}_3$  catalysts.

#### UV-Vis Diffuse Reflectance Spectroscopy (UV-Vis DRS)

The optical properties of the composites were investigated using UV-Vis diffuse reflectance spectroscopy. Spectra were recorded on a UV-Vis spectrophotometer equipped with an integrating sphere, in the wavelength range of 200-800 nm. The optical band gap ( $E_g$ ) was calculated using the Tauc plot method:

where  $a$  is the absorption coefficient,  $h$  is planck's constant,  $\nu$  is the frequency of light, and  $b$  is a constant. This analysis provides insight into the electronic structure of the composites and the influence of ferrocene on light absorption behavior [8].

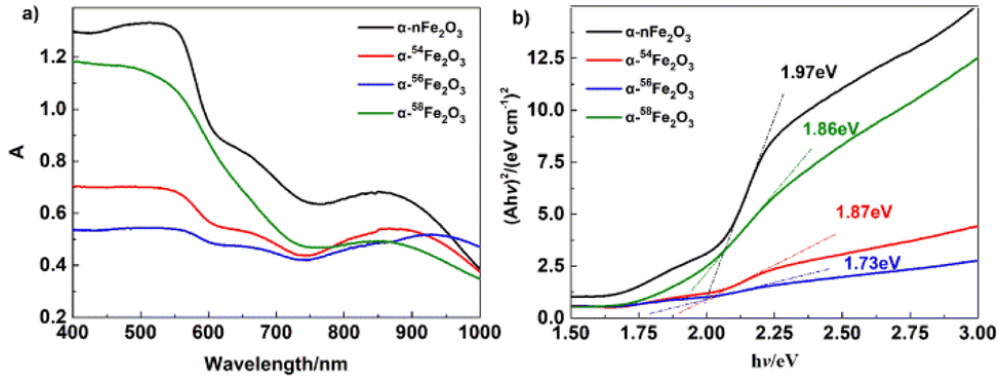


**Fig. 3.** (a) UV-Vis diffuse reflectance spectra of  $\alpha$ - $\text{Fe}_2\text{O}_3$  catalysts, and (b) corresponding Tauc plots for band gap determination.

X-ray Photoelectron Spectroscopy (XPS) – XPS analysis was conducted using an Escalab 250Xi spectrometer with monochromatic Al  $K\alpha$  radiation to determine the surface chemical states of the elements. The binding energies were calibrated using the C 1s peak at 284.8 eV. This technique helps identify chemical interactions between ferrocene and the polymer matrix, particularly the formation of covalent or hydrogen bonds [9]

#### Brunauer-Emmett-Teller (BET) Surface Area Analysis

The specific surface area and pore characteristics of the composites were determined by nitrogen adsorption-desorption isotherms at  $-196^\circ\text{C}$  using an SSA-7000 analyzer. Samples were degassed at  $150^\circ\text{C}$  for 3 hours prior to measurement. The BET method was used to calculate surface area, while the Barrett-Joyner-Halenda (BJH) method was applied for pore size distribution.

Fig 4 and table 2 present the nitrogen adsorption-desorption isotherms and BET surface area data for  $\alpha$ - $\text{Fe}_2\text{O}_3$  catalysts [10]. These results show significantly higher surface areas ( $120 - 145 \text{ m}^2/\text{g}$ ) compared to typical polymer composites, highlighting the potential of iron-based nanoparticles as high-surface-area reinforcements. Such high surface area can promote better interfacial interactions and stress transfer in composite materials.

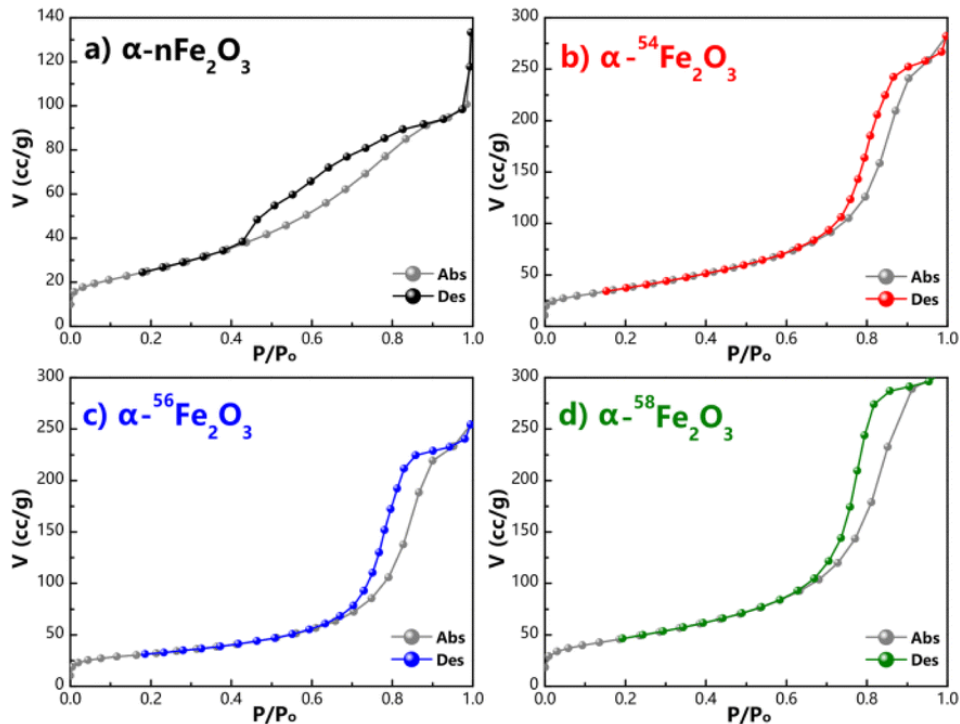


**Fig. 4.** Nitrogen adsorption-desorption isotherms of  $\alpha$ - $\text{Fe}_2\text{O}_3$  catalysts.

### Composition and properties of polymer composites

Polymer matrices can be divided into two main categories: thermosetting and thermoplastic.

**Thermosetting materials:** Once cured, these polymers form a three-dimensional, infusible network. Examples include epoxy resins, unsaturated polyesters, and vinyl esters. When a hardener is added, or upon exposure to heat or UV radiation, an irreversible chemical reaction occurs, often leading to intermolecular crosslinking and the formation of a monolithic, rigid structure. This process is irreversible after completion. Such materials typically exhibit higher stiffness, strength, and heat resistance, but are difficult to reprocess [1].

**Thermoplastics:** In the field of polymeric materials, thermoplastics represent one of the most important and widely used categories, including polypropylene (PP), polyamide (PA), and polyethylene (PE). Thermoplastics exhibit high impact resistance while also being easily recyclable. Thermoplastics are distinguished from other polymeric materials in several aspects, as they can soften at moderately high temperatures and return to their original state upon cooling. This thermoplastic property has increased the utilization of thermoplastics in various industries, including automotive, electronics, packaging, and medical applications.

The choice of matrix depends on the end application. For example, thermosetting epoxy composites are often used in the aerospace industry, while long-fiber-reinforced thermoplastics are increasingly employed in the automotive industry. Table 2 provides a general comparison of the properties of thermosetting and thermoplastic composites [12].

**Table 2.** Comparison of general properties of thermosetting and thermoplastic polymers.

| Property            | Thermosetting plastics (thermosets)          | Thermoplastics               |
|---------------------|--|------------------------------|
| Structure           | Stitched (3D mesh)                           | Linear or branched           |
| Recycling           | Impossible                                   | Possible several times       |
| Thermal stability   | They do not melt and decompose at 200-300°C. | Melts when heated (80-250°C) |
| Mechanical strength | High   | Moderate                     |
| Flexibility         | Low  | High                         |
| Chemical resistance | High   | Average                      |

### Types of reinforcement and their influence on mechanical properties

**Synthetic fiber reinforcement (1-D)-** Fibers are the most common and effective reinforcement for achieving high strength and stiffness, they include natural and synthetic fibers.

Synthetic fibers are engineered for specialized high-performance applications, their primary role is to reinforce a polymer matrix (e.g., epoxy or polyester) and produce composite materials with strength and stiffness significantly superior to those of conventional materials. These fibers bear the applied load, while the matrix holds them in place and distributes stress among them. Glass fibers (E-glass, S-glass), carbon fibers, and aramid fibers (Kevlar, Twaron) provide very high strength and elastic modulus.

Natural fibers such as jute, flax, hemp, and bamboo are attractive due to their good biodegradability, light weight, and low cost. However, they have lower strength and heat resistance than synthetic fibers, and their moisture absorption is problematic. The processes of weaving and forming reinforcing fibers are shown in Fig. 5 [13].

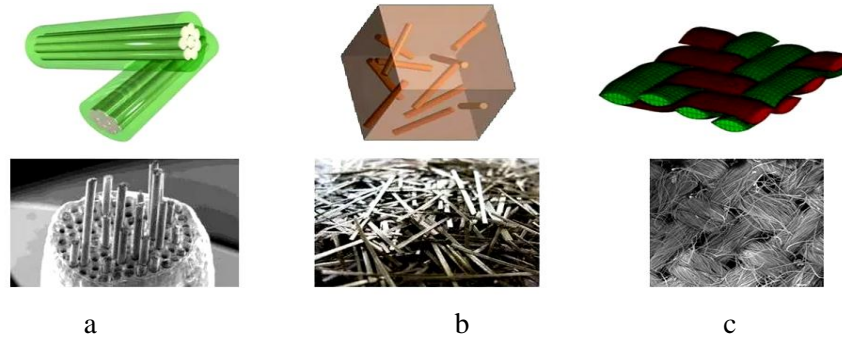


**Fig. 5.** Various fiber weaving and forming processes for use in polymer matrix composites. a) continuous (long) fibers, b) short (chopped) fibers, c) fabric.

The selection of fiber type is one of the most important design parameters for polymer composites. Each fiber type has a unique set of mechanical and physical properties that directly affect the composite's final performance. Key selection criteria include tensile strength, elastic modulus, density, and thermal stability. Table 3 presents relevant properties of several common reinforcing fibers [14].

**Table 3.** Comparison of mechanical properties of some common reinforcing fibers.

| Fiber type         | Density (g/cm <sup>3</sup> ) | Tensile strength (MPa) | Tensile modulus of elasticity (GPa) | Operating temperature range (°C) |
|--------------------|------------------------------|------------------------|-------------------------------------|----------------------------------|
| Glass (E-glass)    | 2.5 - 2.6                    | 2000 - 3500            | 70 - 75                             | Up to ~380                       |
| Carbon (Standard)  | 1.7 - 1.9                    | 3000 - 4000            | 200 - 250                           | Up to ~500 (in vacuum)           |
| Aramid (Kevlar 49) | 1.44                         | 3000 - 3150            | 112 - 124                           | Up to ~250                       |
| Flax               | 1.4 - 1.5                    | 800 - 1500             | 60 - 80                             | -                                |

As shown in table 3, glass and carbon fibers are the most widely used types in various industries such as shipbuilding, aircraft manufacturing, automotive parts and sporting goods due to their low cost and favorable balance of strength and stiffness.

*Two-dimensional (2D) nanomaterials.* Two-dimensional nanomaterials belong to a class of advanced materials with thicknesses ranging from atomic to nanometer scale, but with larger dimensions in the other two directions (from tens of nanometers to several micrometers). The very high aspect ratio and unique layer structure distinguish them from other nanomaterials. The strong interactions and very large surface area of the nanosheets with the polymer matrix provide a very effective reinforcement mechanism that leads to improved mechanical and thermal properties at very low concentrations (even less than 1% wt) [15].

2D nanomaterials, with their unique combination of high aspect ratios, exceptional properties, and performance at low concentrations, constitute a new generation of high-performance polymer composites. Their ability to simultaneously improve multiple properties (mechanical, thermal, barrier, and electrical) makes them an ideal choice for modern applications in the aerospace, electronics, packaging, and energy industries. These include the following:

- Graphene and graphene oxide (GO). They exhibit very high mechanical strength of about (~130 GPa) and thermal conductivity (~5000 W/m \* K).

- Clay nanosheets, such as montmorillonite, are used to improve the barrier properties, flame retardancy, and mechanical properties of composites;

MXenes (pronounced mxenes) are a class of two-dimensional nanomaterials made of transition metal carbides, nitrides, and carbonitrides. They were discovered in 2011 by Yuri Gogotsi and Michel Barsoum.

### Structure

- MXenes consist of layers of transition metals and X-elements, separated by a termination layer. The general formula of these compounds is  $M_n +_1X_nT_n$ , where:

M – is the transition metal;

X – is C, N, and sometimes O;

T – is the termination layer (surface ends) and can consist of *O, OH, F, or Cl*.

### Reinforcing materials based on ferrocene and its compounds

Ferrocene is an orange crystalline organometallic compound with the formula  $Fe(C_5H_5)_2$ , in which

an iron atom is centrally positioned between two aromatic rings (cyclopentadienyl), as shown in Fig. 6.

The distinctive structure of ferrocene consists of a central iron (Fe) atom sandwiched between two parallel planar cyclopentadienyl rings ( $C_5H_5$ ), forming strong bonds between the iron atom and the

carbon atoms of the cyclopentadienyl rings. This creates a stable, symmetrical and aromatic sandwich-like arrangement. This unique structure, known as a metallocene, imparts remarkable stability and reactivity to ferrocene, making it a cornerstone of organometallic chemistry with diverse applications and significantly rendering it a highly attractive reinforcing material for polymer composites.

The aromatic rings of ferrocene can enter into strong  $\pi$ - $\pi$  interactions with other aromatic moieties in the composite, such as graphene, carbon nanotubes, or even benzene rings in the polymer chains. These non-covalent physical interactions provide a secondary and highly effective bonding mechanism that enhances the structural stability of the composite [16].

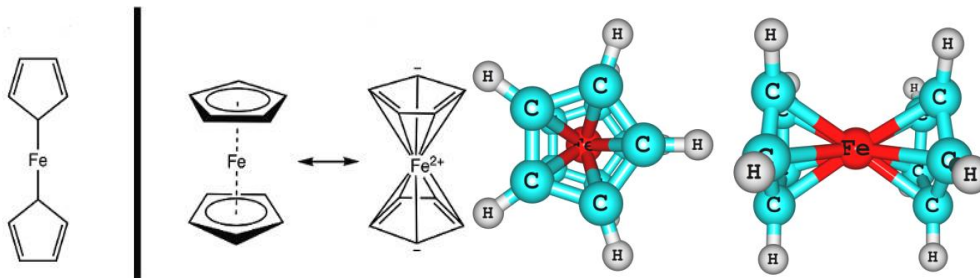


**Fig. 6.** Sandwich structure of the ferrocene molecule  $Fe(C_5H_5)_2$ .

The use of ferrocene based reinforcing materials provides significant thermal stability to the composite (up to approximately  $400^\circ C$ ) due to the organometallic ferrocene rings. Cyclopentadienyl

fragments are easily chemically modified to accommodate various functional groups. This enhances ferrocene's compatibility with various types of polymer matrices (hydrophobic or hydrophilic) and significantly improves interfacial adhesion. For example, an amino group ( $-NH_2$ ) can be introduced to

improve interaction with an epoxy matrix.

Ferrocene derivatives can act as fire retardants the iron in ferrocene promotes the formation of a carbon layer on the surface of the burning polymer, which acts as a thermal barrier and prevents the escape of flammable gases, the addition of only  $3\% wt$  polyferrocene nanoparticles (a ferrocene-based

polymer) to epoxy resin resulted in a 40% increase in fracture toughness and a 25% increase in flexural strength compared to neat epoxy resin.

Another study by Korshak et al. (1987) on polyamide/ferrocene composites showed that these compounds not only improve mechanical strength but also significantly enhance resistance to thermal-oxidative degradation.

Numerous experimental studies demonstrate the high potential of ferrocene-based reinforcing additives for improving the properties of polymer composites. These improvements are not limited to a specific polymer matrix or a single property but are achievable across various polymer systems over a wide range of mechanical and thermal characteristics. Table 4 summarizes the effect of selected ferrocene-based reinforcements on the properties of different polymer composites [17].

**Table 4.** Effect of certain ferrocene-based reinforcing materials on the mechanical properties of polymer composites.

| Polymermatrix | Ferrocene amplifier type                | Added quantity (weight %) | Improving key properties                                     |
|---------------|---|---------------------------|--|
| Epoxy resin   | Polyferrocene                           | 3%                        | +40% crack resistance, +25% bending strength                 |
| Polyamide     | ferrocene                               | 1-5%                      | Improved mechanical strength and oxidative thermal stability |
| Polystyrene   | Ferrocene derivatives with amino groups | 2%                        | Improved interface adhesion and tensile strength             |
| Polyolefin    | Ferrocene oxide nanoparticles           | 4%                        | Improved fire protection properties and thermal stability    |

Ferrocene-based reinforcing agents can improve the mechanical properties of various types of polymer matrices, including thermoset resins (such as epoxy) and thermoplastics (such as polyamide, polystyrene, and polyolefins). From the data presented in Table 4, the following conclusions can be drawn.

The additives influence several properties, including not only mechanical properties (such as strength and impact toughness) but also thermal properties (thermal stability) and even behavioral properties (enhancing fire resistance). The improvement in mechanical properties is primarily attributed to surface-active interactions at the interface (such as covalent bonds) and crack inhibition mechanisms (such as crack bridging and deflection). Even the addition of small amounts (less than 5% wt) of ferrocene-containing reinforcing additives can lead to a significant increase in the physicochemical properties of composites, making their production economically viable while preserving the fundamental properties of the polymer [18].

Therefore, ferrocene and its derivatives can be considered multifunctional and efficient additives for the development of a new generation of polymer composites with improved functional characteristics.

### 3. RESULTS AND DISCUSSION

*Structural analysis by XR* – The crystalline structure of the composites was investigated by X-ray diffraction. Fig 7 shows the XRD patterns of pure polymer matrix and polymer/ferrocene composites with different ferrocene concentrations.

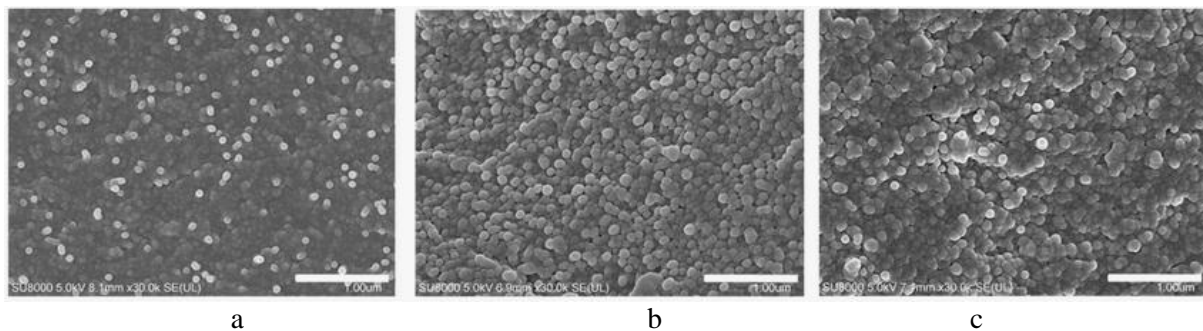


**Fig. 7.** XRD patterns of (a) pure polymer matrix, (b) composite with 1 wt.% ferrocene, and (c) composite with 3% wt. ferrocene.

### Morphological analysis by SEM

The dispersion state of ferrocene particles within the polymer matrix and the interfacial morphology were investigated by SEM. Fig. 7 shows transmission electron microscopy (SEM) images of cryogenically fractured surfaces of the pure polymer and ferrocene-reinforced composites. The SEM images display (a) the pure polymer matrix (smooth surface), (b) the composite with 1% wt ferrocene (partial dispersion), and (c) the composite with 3% wt ferrocene (homogeneous dispersion) [19].

The pure polymer matrix (Fig. 7a) exhibits a relatively smooth and featureless fracture surface, characteristic of brittle fracture. In contrast, the composites containing ferrocene show rougher surfaces with visible particles within the matrix. At 1% wt ferrocene (Fig 7b), some particle agglomeration is observed, indicating non-uniform dispersion. However, at 3% wt ferrocene (Fig 7c), the particles are uniformly distributed throughout the matrix with no significant agglomeration, and the particles are well-embedded with good interfacial contact. This homogeneous dispersion is crucial for effective load transfer from the matrix to the reinforcing particles [20].

### Surface Area and Porosity Analysis by BET

Table 5 presents the BET surface area and pore characteristics of the polymer-ferrocene composites.

The pure polymer exhibits a relatively low surface area of  $5.2 \text{ m}^2/\text{g}$ . Upon the addition of ferrocene, the surface area increases, reaching a maximum of  $6.8 \text{ m}^2/\text{g}$  at a ferrocene content of **3% wt** this increase can be attributed to the creation of additional interfacial area between the polymer matrix and the ferrocene particles. The slight decrease in surface area at 5% wt ferrocene may be due to particle agglomeration, which reduces the effective surface area available for interaction. Meanwhile, the average pore diameter decreases slightly, suggesting that the ferrocene particles either occupy larger pores or create new, smaller pores at the interface [21].

**Table 5.** BET surface area and pore characteristics of polymer/ferrocene composites.

| Sample        | Surface area ( $\text{m}^2/\text{g}$ ) | Average pore diameter (nm) | Pore volume ( $\text{cm}^3/\text{g}$ ) |
|---------------|--|----------------------------|--|
| Pure polymer  | $5.2 \pm 0.3$                          | $12.5 \pm 0.5$             | $0.032 \pm 0.002$                      |
| +1% Ferrocene | $5.8 \pm 0.4$                          | $11.8 \pm 0.4$             | $0.038 \pm 0.003$                      |
| +3% Ferrocene | $6.8 \pm 0.5$                          | $10.2 \pm 0.3$             | $0.045 \pm 0.003$                      |
| +5% Ferrocene | $6.5 \pm 0.4$                          | $10.5 \pm 0.4$             | $0.042 \pm 0.002$                      |

The pure polymer exhibits a relatively low surface area of  $5.2 \text{ m}^2/\text{g}$  upon addition of ferrocene, the surface area increases, reaching a maximum *of*  $6.8 \text{ m}^2/\text{g}$  at 3% wt ferrocene content. This increase can be attributed to the creation of additional interfacial area between the polymer matrix and ferrocene particles. The slight decrease in surface area at 5% wt ferrocene may be due to particle agglomeration, which reduces the effective surface area available for interaction. The pore volume follows a similar trend, while the average pore diameter decreases slightly, suggesting that ferrocene particles occupy larger pores or create new smaller pores at the interface [22].

### XPS Analysis: Chemical Interactions at the Interface

X-ray photoelectron spectroscopy (XPS) was employed to investigate the chemical interactions between ferrocene and the polymer matrix. Fig 9 shows the XPS survey spectra and high-resolution Fe 2p and O 1s spectra for the composite with 3% wt ferrocene. The survey spectrum in Figure 9a confirms the presence of elements C, O, and Fe. The high-resolution Fe 2p spectrum in Fig 9b exhibits two main peaks at **710.9 eV (Fe 2p<sub>3/2</sub>)** and **724.4 eV (Fe 2p<sub>1/2</sub>)**, characteristic of Fe<sup>2+</sup> in ferrocene [23].

### Optical properties and band Gap analysis

The optical properties of the composites were investigated by UV-Vis diffuse reflectance spectroscopy, fig 8a shows the UV-Vis spectra of pure polymer and ferrocene-reinforced composites, while Fig. 8b presents the corresponding Tauc plots for band gap determination.

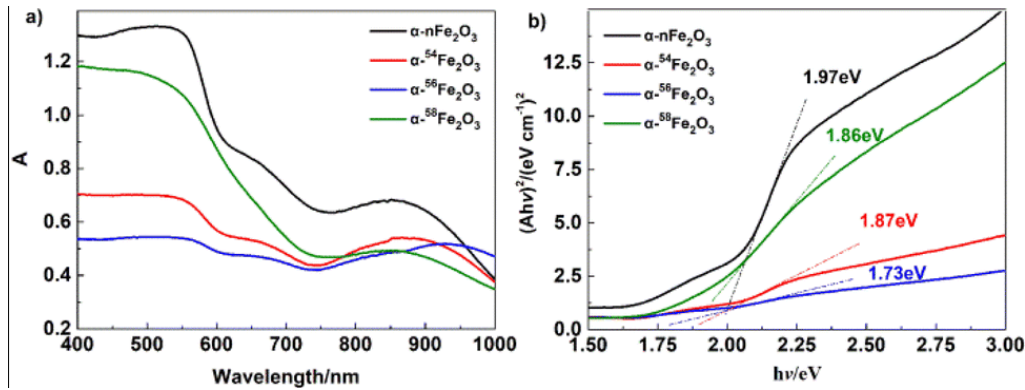


**Fig. 8.** UV-Vis diffuse reflectance spectra of pure polymer and polymer/ferrocene composites and (b)  $(Ah\nu)^2$  vs  $h\nu$  plots for band gap calculation.

**Table 6.** Band gap values ( $E_g$ ) and catalytic results of  $\alpha$ - $\text{Fe}_2\text{O}_3$  on the thermal decomposition of AP.

| Compound                                    | $T_{\text{endo}}/^\circ\text{C}$ | RSD   | $T_{\text{exo}}/^\circ\text{C}$ | RSD   | $E_g/\text{eV}$ |
|---|----------------------------------|-------|---------------------------------|-------|-----------------|
| AP  | 242.50                           | 0.28% | 439.76                          | 0.21% | —               |
| $\alpha$ - $n\text{Fe}_2\text{O}_3$ /AP     | 242.59                           | 0.08% | 341.34                          | 0.47% | 1.97            |
| $\alpha$ - $^{54}\text{Fe}_2\text{O}_3$ /AP | 243.36                           | 0.11% | 341.98                          | 0.32% | 1.87            |
| $\alpha$ - $^{56}\text{Fe}_2\text{O}_3$ /AP | 243.20                           | 0.15% | 346.25                          | 0.32% | 1.73            |
| $\alpha$ - $^{58}\text{Fe}_2\text{O}_3$ /AP | 243.95                           | 0.11% | 344.34                          | 0.16% | 1.86            |

The pure polymer exhibits an absorption edge at approximately 350 nm, corresponding to a band gap of about 3.54 eV. Upon the addition of ferrocene, the absorption edge shifts to longer wavelengths (red shift), indicating a reduction in the band gap. The calculated band gap values, obtained from Tauc plots, are summarized in table 6.

The flexural strength of the composites, measured by three-point bending test, is presented in Table 7, the flexural strength follows a similar trend to tensile properties, with maximum value achieved at 3% wt ferrocene content [24].

**Table 7.** Summary of mechanical properties of polymer/ferrocene composites.

| Sample        | Tensile strength (MPa) | Elastic modulus (GPa) | Elongation at break (%) | Flexural strength (MPa) |
|---------------|------------------------|-----------------------|-------------------------|-------------------------|
| Pure polymer  | $56.0 \pm 2.1$         | $1.8 \pm 0.1$         | $5.2 \pm 0.3$           | $85.0 \pm 3.0$          |
| +1% Ferrocene | $68.5 \pm 2.5$         | $2.1 \pm 0.1$         | $4.8 \pm 0.2$           | $98.0 \pm 3.5$          |
| +3% Ferrocene | $78.0 \pm 2.8$         | $2.5 \pm 0.2$         | $4.1 \pm 0.2$           | $112.0 \pm 4.0$         |
| +5% Ferrocene | $75.0 \pm 3.0$         | $2.4 \pm 0.2$         | $3.5 \pm 0.3$           | $108.0 \pm 4.0$         |

The improvement in mechanical properties can be attributed to several factors, first the uniform dispersion of ferrocene particles within the polymer matrix, ensures effective load transfer from the matrix to the rigid ferrocene particles. Second the strong interfacial adhesion between ferrocene and the polymer matrix, facilitated by  $\pi$ - $\pi$  interactions between the aromatic rings of ferrocene and aromatic groups in the polymer chain (if present), enhances stress transfer efficiency. Third the crystalline nature of ferrocene, as confirmed by XRD, contributes to the overall stiffness of the composite [25].

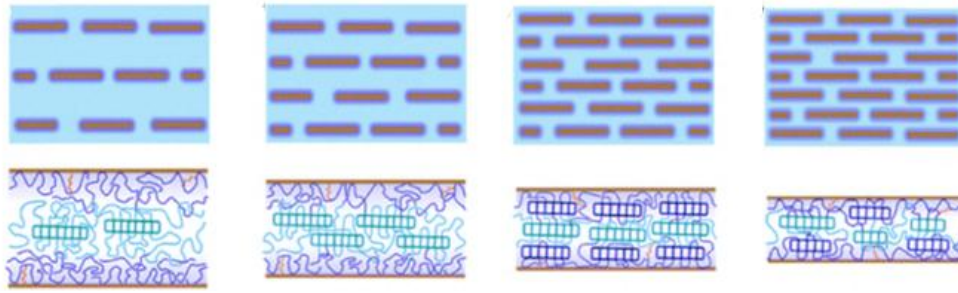


**Fig. 9.** representation of the proposed reinforcement mechanism: (a) pure polymer matrix with chain entanglements, (b) incorporation of ferrocene particles showing  $\pi$ - $\pi$  interactions with polymer chains, and (c) load transfer mechanism under tensile stress.

As illustrated in Fig. 9 ferrocene particles act as physical crosslinking points within the polymer matrix. Under applied stress these particles hinder polymer chain mobility and deflect crack propagation, leading to increased strength and modulus. The slight reduction in elongation at break indicates that the material becomes more rigid and less ductile upon ferrocene addition.

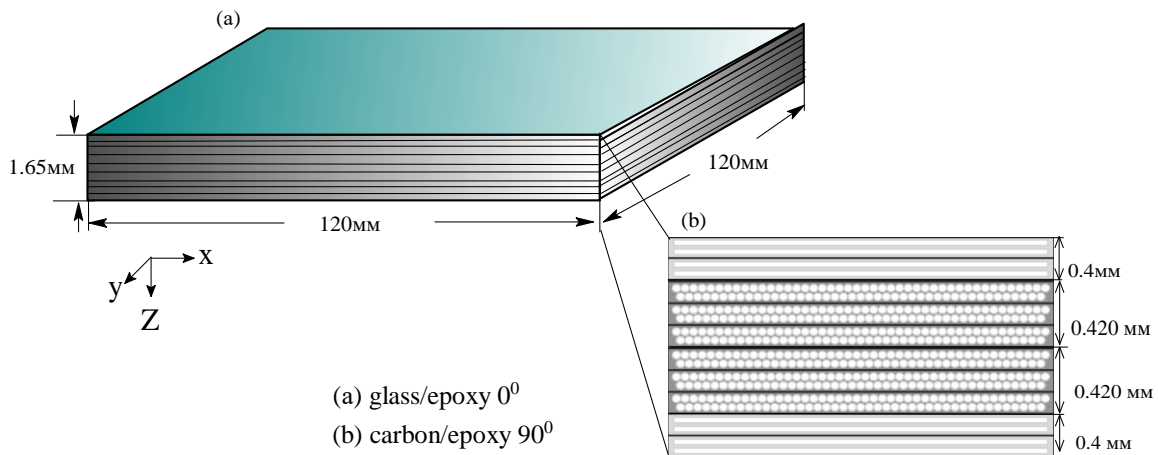
The decrease in properties at 5% wt ferrocene content is likely due to particle agglomeration at higher concentrations, which creates stress concentration points and weakens the composite structure. This finding highlights the importance of optimizing the reinforcement content for maximum performance [26].

### Hybrid composites

Hybrid composites are a class of multifunctional materials used for creating modern structural elements. Their primary application is when a combination of several characteristics is required, such as high mechanical strength and electrical or thermal conductivity. These composites are fabricated using two main methods: either one type of reinforcing material is introduced into a polymer matrix, or a specific polymer matrix is reinforced with several types of reinforcing materials [27].

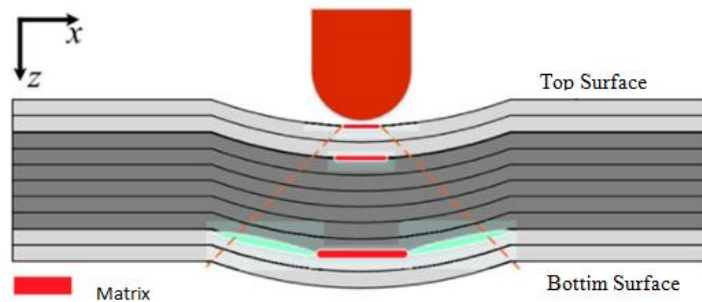
The goal of developing these materials is the intelligent combination of two or more different reinforcements to leverage the advantages of each while simultaneously compensating for their drawbacks, ultimately achieving an optimal balance of physical and mechanical properties. In a hybrid composite, glass fiber can provide overall strength and the primary framework, while ferrocene nanoparticles improve the interfacial adhesion between the fibers and the matrix, leading to increased fracture toughness.

Fig. 10 shows a schematic view of the structure of a hybrid composite, as can be seen, macro- (carbon/glass fibers) and nano- (nanoparticles, carbon nanotubes/graphene sheets) reinforcing additives are simultaneously dispersed within the polymer matrix. This hybrid structure, by creating a synergy between reinforcement mechanisms at different scales, leads to a simultaneous improvement in mechanical, thermal, and electrical properties [28].



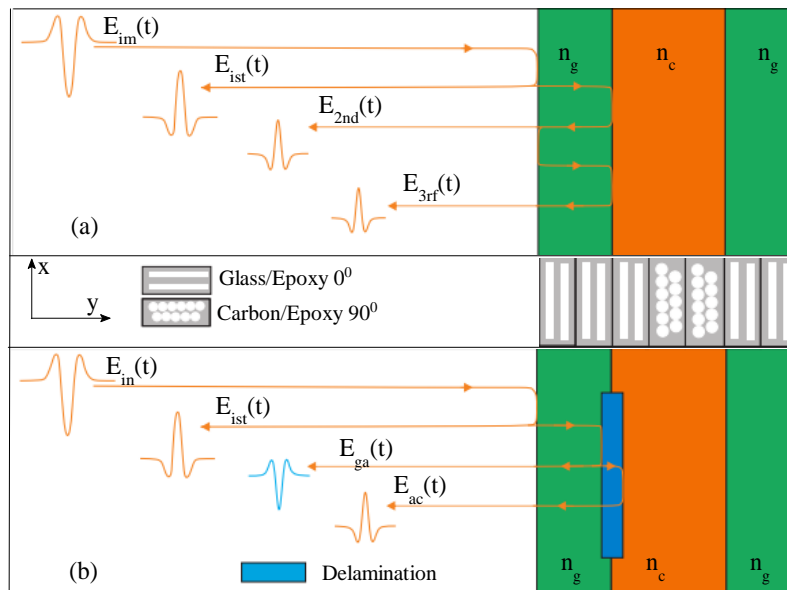
**Fig. 10.** Schematic representation of a hybrid composite structure.

Fig. 11. Shows an edge view of the same specimen after it was subjected to low-velocity impact, showing various types of damage such as matrix cracking, fiber delamination.



**Fig. 11.** Schematic diagram (edge view) of a sample subjected to low-velocity impact with highlighted damage types.

For non-destructive testing and the detection of such internal damage, the terahertz (THz) testing method is used. Fig. 11 presents the results of this assessment, including the expected reflected terahertz waveforms in an undamaged area (a) and in an area with delamination (b). A comparison of these two waveforms allows for the precise detection and localization of the damaged area. In this testing method, a photoconductive antenna is used to generate short terahertz pulses. This emitter utilizes the photoconductive effect in a semiconductor to convert incoming laser beams into terahertz pulses. The signals reflected from the sample are then received by a terahertz detector. By analyzing the changes in the amplitude, phase, and time delay of these signals relative to a reference signal, accurate information can be obtained about the depth, size and nature of internal damage, including delamination and cracks [29].



**Fig. 12.** Calculated forms of reflected terahertz waves in an undamaged area (a) and in a delamination area (b).

In this schematic structure, macrofibers act as the primary load-bearing scaffold, while nanofillers significantly increase the strength and modulus of the composite by filling the spaces between the fibers and improving fiber-matrix bonding. Evaluating the behavior of these advanced composites under load, including their resistance to impact damage is important.

Other commonly used hybrid combinations include:

- Graphene/ferrocene derivatives: Ferrocene derivatives can act as coupling agents between inert graphene sheets and the polymer matrix, improving the uniform dispersion of graphene and leading to enhanced mechanical and electrical properties.
- Natural fibers/ferrocene derivatives: Ferrocene derivatives significantly reduce the moisture absorption of hydrophilic natural fibers by forming a hydrophobic layer on their surface. This increases the stability and substantially extends the strength and service life of the composite in humid environments [30].

### Important mechanical parameters and testing of polymer composites.

Mechanical research and testing are crucial for determining the performance parameters, range, and capabilities of composites. Identifying these properties and characteristics is essential for understanding the required specifications, deformation, and various failure modes of this class of materials, as this directly impacts the design of final products and their applications. Developing the necessary mechanical tests to understand the behavior of these materials under load and their failure ensures that the component will perform adequately in specific industrial conditions [31].

Typical mechanical tests for polymer composites include:

**1. Uniaxial tensile test (ASTM D638)** – A composite specimen of specified dimensions and shape is placed in a tensile testing machine, and a stress–strain curve is recorded, describing the material's behavior under tension until failure. Yield strength, tensile strength, toughness, and elastic modulus are determined.

**2. Three-point bending test (ASTM D790)** – Composites and thermoplastic materials are subjected to bending loads; their surfaces and edges experience tensile or compressive stresses depending on the direction of load application. For most polymer composites, compressive strength in this test is lower than tensile strength, and specimens fail more rapidly on the compression side. This failure is caused

by the formation of microkinks on the compressed surface and is related to the properties of the reinforcing materials [32].

**3. Four-point bending test (ASTM D6272)** – This test determines the flexural modulus under bending, torsion, and twisting stresses. It is similar to the three-point bending test, except that four support points are used instead of three, and the load is applied through two points. This results in a more uniform stress distribution, making it more suitable for brittle materials. Another key difference is the absence of shear stresses within the specimen [33].

**4. Poisson's ratio test (ASTM D3039)** – An important parameter used in structural design that allows assessment of dimensional changes under applied stress and the occurrence of deformations. This test evaluates deformations occurring in directions perpendicular to the applied load.

**5. Flat compression test (ASTM C365)** – Determines the compressive strength of components used as sandwich structures in construction.

**6. Combined loading compression test (ASTM D6641)** – Used to study the stiffness and strength of a specimen. The test involves subjecting the specimen to both shear stress and compressive load.

**7. Fatigue test (ASTM D7791)** - Describes the fatigue behavior of plastics under uniaxial loading. Surface conditions, stresses, and other specimen characteristics influence the fatigue strength of plastics and their reinforcing elements when subjected to a large number of loading cycles [34].

### Mechanical properties of composites depending on the type of reinforcement used

**Fiber-reinforced polymer composites.** In recent years, fiber-reinforced composites have gained widespread recognition due to their low weight, affordable cost, and excellent mechanical properties and strength. Researchers have conducted numerous research projects on these materials. Numerous studies have examined the mechanical properties of fiber-reinforced composites as a function of the amount of carbon fiber added to the matrix, as well as the size, diameter, and shape of the fibers added to the matrix phase.

One study examined the effect of adding carbon fibers on the mechanical and electrical properties of polypropylene-based composites. Composite samples with varying fiber contents (5, 10, and 15% wt) were fabricated and tested for tensile strength, tensile modulus, and impact toughness. Analysis of the results showed that increasing the reinforcement content led to an increase in all of the aforementioned mechanical properties. The best result was obtained for the sample containing 15% wt carbon fibers, which exhibited a tensile strength of 98 MPa and a tensile modulus of 4.14 GPa.

The addition of natural pineapple fibers to polyester-based composites was also studied. Mechanical testing of the prepared samples showed that increasing the fiber content significantly increased compressive, flexural, and tensile strengths. Detailed data are presented in table 8 [35].

**Table 8.** Investigation of mechanical properties of some fiber-reinforced polymer composite materials.

| Composite                        | Density(g/cm) | Strain increase(%) | Tensile strength (MPa) | Young's modulus (GPa) |
|----------------------------------|---------------|--------------------|------------------------|-----------------------|
| Epoxy +40% Sisal fibers          | -             | -                  | 56                     | -                     |
| Polyamide + 20-30% carbon fiber  | 1.38-1.68     | 0.8-5.5            | 36.5-241               | 4.5-29                |
| Polypropylene + 20% glass fibers | 1.03          | 43                 | 100                    | 4.3                   |
| Polypropylene + 40% glass fibers | 1.22          | 2                  | 127                    | 7.6                   |
| Polypropylene + 30% carbon fiber | 1.07          | 1                  | 117                    | 16.2                  |
| Polypropylene + 30% linen fibers | -             | -                  | 58.5                   | 4.1                   |
| Vinyl ester + carbon fiber       | 1.50-1.65     | 1.4                | 900-1200               | 1.36                  |
| Vinyl ester + 24% linen fiber    | -             | -                  | 248                    | 24                    |
| Vinyl ester + 59% glass fiber    | -             | -                  | 483                    | 33                    |
| Vinyl ester + Kevlar fiber       | 1.35          | -                  | 500                    | 40                    |
| Epoxy + Kevlar + 20% Hemp fibers | 1.46          | -                  | 95                     | -                     |

### Reinforcement mechanisms and structure-property relationships

The experimental results presented in this review demonstrate that ferrocene-based reinforcements significantly enhance the mechanical properties of polymer composites through multiple mechanisms. The uniform dispersion of ferrocene particles, confirmed by SEM and BET analysis, ensures efficient stress transfer from the polymer matrix to the rigid ferrocene domains. The strong interfacial adhesion, evidenced by XPS and FTIR, facilitates load transfer through chemical interactions ( $\pi$ - $\pi$  stacking) and physical interlocking.

The crystalline structure of ferrocene, confirmed by XRD, contributes to the overall stiffness of the composite, as crystalline domains typically have higher modulus than amorphous polymer regions. The reduction in optical band gap upon ferrocene addition suggests the formation of charge-transfer complexes, which may also influence mechanical behavior by altering the electronic structure of the matrix.

The optimal reinforcement content (3 wt% in this case) represents a balance between the benefits of uniform dispersion and the drawbacks of agglomeration at higher loadings. At 5% wt ferrocene, particle agglomeration creates stress concentration points that initiate failure, leading to reduced mechanical properties. This trend is consistent with observations in other nanoparticle-reinforced systems [36].

### Comparative Analysis with Iron Oxide Nanostructures:

On  $\alpha$ - $\text{Fe}_2\text{O}_3$  catalysts provides valuable insights into the structure-property relationships of iron-based materials. Although their study focused on catalytic activity rather than mechanical reinforcement, several parallels can be drawn:

**1. Crystalline Structure:** Both ferrocene and  $\alpha$ - $\text{Fe}_2\text{O}_3$  exhibit well-defined crystalline structures (figure 1a vs. Reference Fig 1a), which is essential for effective load transfer in composites.

**2. Surface Morphology:** The rough surface morphology of iron oxide nanoparticles (reference Fig 1b) promotes mechanical interlocking with polymer matrices, a mechanism that also operates in ferrocene-based composites (fig 1b).

**3. Surface Area:** The significantly higher surface area of iron oxide nanoparticles (Table 2) suggests that incorporating such high-surface-area materials as hybrid reinforcements could further enhance mechanical properties through improved interfacial interactions.

**4. Chemical Bonding:** The similar Fe 2p binding energies observed in both systems (fig 1e vs. Reference Fig 1e) confirm the stability of iron-centered structures in polymer matrices.

**5. Optical Properties:** The lower band gap of iron oxides (fig 1d) compared to ferrocene composites indicates different electronic structures, which may be exploited for multifunctional applications requiring specific optical or electronic properties.

These comparisons highlight the potential for developing hybrid composite systems that combine the unique organometallic properties of ferrocene with the high surface area and catalytic activity of iron oxide nanoparticles. Such hybrid reinforcements could lead to composites with simultaneously enhanced mechanical, thermal, and functional properties [37].

## 4. CONCLUSIONS

This review clearly demonstrates that polymer composites have established themselves as a preferred choice in advanced industries due to their high strength to weight ratios and design flexibility. The mechanical properties of these materials depend significantly on the type, dispersion and content of the reinforcing phase. Therefore, various reinforcement types ranging from micro and nanoparticles to fibers and two-dimensional nanomaterials have been investigated.

The results of this systematic review indicate that ferrocene compounds have emerged as innovative and highly effective reinforcing nanomaterials owing to their unique sandwich structure, high thermal stability, and ability to form strong  $\pi$ - $\pi$  interactions. These compounds can significantly enhance the fracture toughness, flexural strength, and impact resistance of the final composite by improving adhesion at the interface between the polymer matrix and other reinforcements (fibers or graphene). Furthermore, the presence of metallic iron in their structure imparts flame-retardant properties.

Comprehensive characterization using XRD, SEM, BET, XPS, and UV-Vis DRS has provided detailed insights into the structure-property relationships in ferrocene-reinforced composites. The optimal reinforcement content of 3% wt achieves uniform dispersion, strong interfacial adhesion, and enhanced mechanical properties, while higher loadings lead to agglomeration and property degradation. The reduction in optical band gap upon ferrocene addition suggests potential for multifunctional applications combining mechanical reinforcement with tailored optical properties.

A comparative analysis with iron oxide nanostructures reveals that iron-based reinforcements share common characteristics such as crystalline structure, surface roughness and chemical stability, while exhibiting distinct differences in surface area and electronic properties. This comparison opens new avenues for developing hybrid composite systems that leverage the advantages of both organometallic ferrocene and inorganic iron oxides.

Moreover, the development of hybrid composites through the judicious combination of multiple reinforcing components is a key strategy for achieving an optimal balance of properties and overcoming the limitations of single-component systems. In this context, ferrocene derivatives can act as effective coupling agents, providing excellent mechanical performance and versatility.

In summary ferrocene-based reinforcing materials with their unique set of properties, possess high potential for substantially improving the next generation of polymer composites and expanding their application scope in sensitive and advanced industrial sectors.

## REFERENCES

1. Callister Jr. W.D., Rethwisch D.G. *Materials science and engineering: an introduction*. John Wiley & sons. 2020.
2. Khabrat Gh.R., Puzin Y.I. Ferrocene-containing compounds as combustion catalysts and solid fuel modifiers. *Construction materials and products*. 2025. 8 (3). P. 6. DOI: 10.58224/2618-7183-2025-8-3-6.
3. Saltykova S.N., Karapetyan K.G., Korshunov A.D., Nazarenko M.Yu., Dorosh I.V. Adsorption properties of oil shale ash residues of leningradskoye field. *Sorbtsionnye i khromatograficheskie protsessy*. 2024. 24 (6). P. 1003 – 1014. (In Russ.) DOI: 10.17308/sorpchrom.2024.24/12587.
4. Mohammed L., Ansari N.M.N., Pua G., Jawaid M., Islam M.S. Review on natural fiber reinforced polymer composite and its applications. *International Journal of Polymer Science*. 2015. 2015 (243947). DOI: 10.1155/2015/243947.
5. Xiao S., Xue Y., Zhao J., Liu X., Cong H., Lan T., Ouyang Y. Differences in the catalytic properties of Fe isotopes. *RSC advances*. 2023. 13 (35). P. 24812 – 24818. DOI: 10.1039/D3RA04247A.
6. Gunnemann C., Bahnemann D.W., Robertson P.K.J. Isotope effects in photocatalysis. *ACS Omega*. 2021. 6 (17). P. 11113 – 11121. DOI: 10.1021/acsomega.1c00745.
7. Das P.P., Chaudhary V., Ahmad F., Manral A. Effect of nanotoxicity and enhancement in performance of polymer composites using nanofillers: A state-of-the-art review. *Polymer Composites*. 2021. 42 (5). P. 2152 – 2170. DOI: 10.1002/pc.25968.
8. Amin B.U., Yu H., Wang L., Fahad S., Nazir A., Haq F., Liang R. Synthesis and antimigration studies of ferrocenebased amides as burning rate catalysts. *Journal of inorganic and organometallic polymers and materials*. 2021. 31. P. 2511 – 2520. DOI: 10.1007/s10904-020-01861-7.
9. Pickering K.L., Aruan Efendy M.G., Le T.M. A review of recent developments in natural fibre composites and their mechanical performance. *Composites part A: Applied science and manufacturing*. 2016. 83. P. 98 – 112. DOI: 10.1016/j.compositesa.2015.08.038
10. Yan L., Chouw N., Jayaraman K. Flax fibre and its composites – A review. *Composites part B: Engineering*. 2014. 56. P. 296 – 317. DOI: 10.1016/j.compositesb.2013.08.014
11. 5Kausar A. Role of thermosetting polymer in structural composite. *Am. J. Polym. Sci. Eng*, 5 (1), 1-12. (2017). DOI://www.ivyunion.org/
12. Astruc D. Why is ferrocene so exceptional? *European Journal of Inorganic Chemistry*. 2017. 2017 (1). P. 6 – 29. DOI: 10.1002/ejic.201600983

13. Hailes R.L., Oliver A.M., Gwyther J., Whittell G.R., Manners I. Polyferrocenylsilanes: synthesis, properties, and applications. *Chemical Society Reviews*. 2016. 45 (19). P. 5358 – 5407. DOI: 10.1039/C6CS00155F
14. Beitollahi H., Khalilzadeh M.A., Tajik S., Safaei M., Zhang K., Jang H.W., Shokouhimehr M. Recent advances in applications of voltammetric sensors modified with ferrocene and its derivatives. *ACS omega*. 2020. 5 (5). P. 2049 – 2059. DOI: 10.1021/acsomega.9b03788
15. Aydemir T., Golubeva N.D., Shershneva I.N., Kydralieva K.A., Dzhardimalieva G.I. Formation, structure and magnetic properties of nanocomposites obtained by Fe (III) Co (II) cocrystallized complexes thermal decomposition. *Aerospace MAI Journal*. 2019. 26 (2). P. 219 – 228.
16. Shu-hong B., Si-yu C., Lu F. Recent advances in ferrocene-based burning rate catalysts for solid propellants. *Chinese Journal of Energetic Materials*. 2021. 29 (5). P. 460 – 470. DOI: 10.11943/CJEM2021023.
17. Wan C., Duan H., Zhang C., Cao J., Zou J., Zhang J., Ma H. AP/N/S-containing compound toward enhanced fire safety epoxy resin with well-balanced performance. *Polymer Degradation and Stability*. 2021. 192 (109698). DOI: 10.1016/j.polymdegradstab.2021.109698.
18. Kotal M., Bhowmick A.K. Polymer nanocomposites from modified clays: Recent advances and challenges. *Progress in Polymer Science*. 2015. 51. P. 127 – 187. DOI:10.1016/j.progpolymsci.2015.10.001
19. Shojaee Barjoe S., Rodionov V., Babkin R., Tumanov M., Shojaee Barjoe B. An Integrated Modified Failure Mode Effects Analysis Shannon Entropy Combined Compromise Solution Approach to Safety Risk Assessment in Stone Crusher Unit of Ceramic Sector. *International Journal of Engineering*. 2025. 39 (8). P. 1976 – 1987. DOI: 10.5829/ije.2026.39.08b.15
20. Lin L., Gu C., Zhu J., Ye Q., Jiang E., Wang W., Zhu Y. Engineering of hole-selective contact for high-performance perovskite solar cell featuring silver back-electrode. *Journal of Materials Science*. 2019. 54 (10). P. 7789 – 7797. DOI: 10.1007/s10853-018-03258-x
21. Sanjay M.R., Madhu P., Jawaid M., Senthamaraiannan P., Senthil S., Pradeep S. Characterization and properties of natural fiber polymer composites: A comprehensive review. *Journal of Cleaner production*. 2018. 172. P. 566 – 581. DOI: 10.1016/j.jclepro.2017.10.101
22. Amir A., Porwal H., Mahalingam S., Wu X., Wu T., Chen B., Edirisinghe M. Microstructure of fibres pressure-spun from polyacrylonitrile–graphene oxide composite mixtures. *Composites Science and Technology*. 2020. 197 (108214). DOI: 10.1016/j.compscitech.2020.108214
23. Puzin P.Yu., Puzin Yu.I. Influence of ferrocene on solution polymerization of methyl methacrylate. *SOCAR Proceedings*. 2022. (1). P. 1 – 5. DOI: 10.5510/OGP202201100650
24. Seydibeyoğlu M.Ö., Dogru A., Wang J. et al. Review on hybrid reinforced polymer matrix composites with nanocellulose, nanomaterials, and other fibers. *Polymers*. 2023. 15 (4). P. 984. DOI: 10.3390/polym15040984
25. Sathish S., Nirmala R., Kim H.Y., Navamathavan R. Deriving activated carbon using microwave combustion technique and its energy storage applications: a topical review. *Carbon Letters*. 2022. 32 (5). P. 1151 – 1171. DOI: 10.1007/s42823-022-00348-4
26. Valerievna K.E., Vladimirovna Z.O., Yurievich B.V. Involvement of products of chemical processing of polymer waste in the composition of building Materials. *Egyptian Journal of Petroleum*. 2024. 33 (3). P. 441 – 449. DOI: 10.62593/2090-2468.1039
27. Zgonnik P.V., Kuzhaeva A.A. The study of metal corrosion resistance near weld joints when erecting building and structures composed of precast structures. *Applied Sciences (Switzerland)*. 2022. 12 (5). P. 2518. DOI: 10.3390/app12052518
28. Ketova Y.A., Bai B., Khizhnyak G.P., Gladkikh Y.A., Galkin S.V. Testing of preformed particles polymer gel technology on core filtration models to limit water inflows. *Journal of Mining Institute*. 2020. 241. P. 91 – 98. DOI: 10.31897/pmi.2020.1.91

29. Morenov V., Leusheva E., Lavrik A., Lavrik A., Buslaev G. Gas-Fueled Binary Energy System with Low-Boiling working fluid for enhanced power generation. *Energies*. 2022. 15 (7). 2551. DOI: 10.3390/en15072551
30. Cheremisina O.V., Ponomareva M.A., Molotilova A.Yu., Mashukova Yu.A., Solovev M.A. Sorption purification of acid storage facility water from iron and titanium on organic polymeric materials. *Journal of Mining Institute*. 2023. 264. P. 971 – 980. DOI: 10.31897/PMI.2023.28
31. Buslaev G., Lavrik A., Lavrik A., Tsvetkov P. Hybrid system of hydrogen generation by water electrolysis and methane partial oxidation. *International Journal of Hydrogen Energy*. 2023. 48 (63). P. 24166 – 24179. DOI: 10.1016/j.ijhydene.2023.03.098
32. Wang L., Yu H., Saleem M., Akram M., Abbasi N.M., Khalid H., Chen Y. Ferrocene-based polyethyleneimines for burning rate catalysts. *New Journal of Chemistry*. 2016. 40 (4). P. 3155 – 3163. DOI: 10.1039/C5NJ03301A
33. Seydibeyoğlu M.Ö., Dogru A., Wang J., Rencheck M., Han Y., Wang L., Gardner D.J. Review on hybrid reinforced polymer matrix composites with nanocellulose, nanomaterials, and other fibers. *Polymers*. 2023. 15 (4). 984. DOI: 10.3390/polym15040984
34. Strokova V.V., Gubareva E.N., Ogurtsova Yu.N., Nerovnaya S.V. On the possibility of utilization of carbonate-containing mining waste by producing photocatalytic composite materials. *Journal of Mining Institute*. 2025. 276 (2). P. 29 – 41.
35. Sayam A., Rahman A.M., Rahman M.S., Smriti S.A., Ahmed F., Rabbi M.F., Faruque M.O. A review on carbon fiber-reinforced hierarchical composites: mechanical performance, manufacturing process, structural applications and allied challenges. *Carbon Letters*. 2022. 32 (5). P. 1173 – 1205. DOI: org/10.1007/s42823-022-00358-2
36. Kogan V.E., Zgonnik P.V., Shakhparonova T.S., Sobianina D.O., Suvorova Z.V. The physicochemical bases of oil and oil products absorption by glassy sorbents. *Rasayan Journal of chemistry*. 2021. 14 (3). P. 2006 – 2016. DOI: 10.31788/RJC.2021.1435750
37. Gerasimov A.M. Influence of Thermal Modification on the Separation Processes of Clay-Containing Waste Suspensions. *Journal of Ore Beneficiation*. 2022. (1). P. 57 – 59 DOI: //www.rudmet.ru/journal/2108/article/35197/

### INFORMATION ABOUT THE AUTHORS

**Puzin Y.I.**, email: ppuziny@mail.ru, ORCID ID: <https://orcid.org/0000-0003-0756-2666>, SCOPUS: <https://www.scopus.com/authid/detail.uri?authorId=6701395498>, Empress Catherine II Saint Petersburg Mining University, Doctor of Chemical Sciences (Advanced Doctor), Professor

**Khabrat Gh.R.**, e-mail: khabrat2022@gmail.com / s223217@stud.spmi.ru, ORCID ID: <https://orcid.org/0009-0002-5833-8752>, Empress Catherine II Saint Petersburg Mining University, Candidate of at Chemical Sciences (PhD), Engineering and Energy Processing Department